

## Role of viscous friction in the reverse rotation of a disk

Pablo de Castro\* and Fernando Parisio†

*Departamento de Física, Universidade Federal de Pernambuco, 50670-901, Recife, Pernambuco, Brazil*

(Received 23 September 2013; revised manuscript received 20 May 2014; published 22 July 2014)

The mechanical response of a circularly driven disk in a dissipative medium is considered. We focus on the role played by viscous friction in the spinning motion of the disk, especially on the effect called reverse rotation, where the intrinsic and orbital rotations are antiparallel. Contrary to what happens in the frictionless case, where steady reverse rotations are possible, we find that this dynamical behavior may exist only as a transient when dissipation is considered. Whether or not reverse rotations in fact occur depends on the initial conditions and on two parameters, one related to dragging, inertia, and driving, the other associated with the geometric configuration of the system. The critical value of this geometric parameter (separating the regions where reverse rotation is possible from those where it is forbidden) as a function of viscosity is well adjusted by a  $q$ -exponential function.

DOI: [10.1103/PhysRevE.90.013201](https://doi.org/10.1103/PhysRevE.90.013201)

PACS number(s): 45.20.dc, 45.40.Bb, 81.40.Pq

### I. INTRODUCTION

Classical mechanics of simple, low-dimensional, and integrable systems can be surprisingly rich, provided that nonlinearity is present. These systems, although less complex than the chaotic ones, hardly allow for full analytical treatments and may present behaviors like reverse rotations, excitability, transients, and hysteresis, thus constituting an important resource in basic physics. Not less importantly, for obvious reasons, all sorts of machinery in industries work in nonchaotic regimes, however, displaying a variety of complex dynamical effects arising from nonlinearities.

One class of problems that has been often considered in the literature is that of rigid body dynamics on flat surfaces. Farkas *et al.* have explored the subtle connection between translational and spinning motions of a free disk (of radius  $R$ ) moving on a surface with Coulombian friction [1]. They showed, e.g., that the terminal translational ( $v$ ) and rotational ( $\Omega$ ) velocities vanish simultaneously, and that the ratio  $\epsilon = v/R\Omega$  always tends to  $\approx 0.653$  in the imminence of stopping, no matter its initial value (see also [2,3]). Complementarily, the motion of driven disks sliding on frictionless surfaces has been shown to be quite nontrivial regarding a dynamical behavior called reverse rotation [4].

The position of a rigid body in two dimensions is completely characterized by the location of its center of mass (c.m.) and by the angle between some reference line marked on the body and an arbitrary coordinate axis. A reverse rotation develops when the c.m. follows a bounded trajectory in, say, the clockwise direction and, at the same time, the intrinsic angular degree of freedom evolves counterclockwise, or vice versa. Thus, a reverse rotation is characterized by antiparallel orbital and spin rotations. Famous examples of such a phenomenon are the reverse, or retrograde, rotations of Venus [5–7] and Uranus [5]. Behaviors belonging to the same class can be found in the dynamics of rolling cylinders immersed in viscous fluids [8–10] and in the chaotic response of a damped pendulum parametrically excited [11].

From a more applied point of view, reverse rotations may appear, being potentially deleterious, in bearings of journal machinery used to produce newspaper in large scale [12]. They also seem to be relevant in the problem of biological tissue production, where a commonly used method to generate tissue is the rotating vessel bioreactor. It consists of a cylindrical container rotating about its longitudinal axis with constant angular speed. A porous disk is seeded with cells to be cultured and placed within the bioreactor which, in turn, is filled with a nutrient-rich medium. The rotating fluid keeps the growing tissue construct suspended against gravity and leads to intricate dynamical regimes. Various studies on the orbits described by the disk exist [13,14]. Although this system is not identical to the one we study here, it is clear that a better understanding of the regimes of intrinsic rotation, in the spirit of the present work, is needed. For example, the existence of a transient between two distinct spinning regimes, like the one we find here, would produce “topological” defects in the tissue.

In this work we consider both driving and friction simultaneously. Our main goal is to understand how the presence of viscous friction affects the regimes of reverse rotation that have been shown to exist for circularly driven disks in the nondissipative case [4]. Hereafter we refer to the regime where both angular momenta are parallel as normal or prograde.

### II. SYSTEM AND EQUATION OF MOTION

Our model system is depicted in Fig. 1. It consists of a uniform disk of mass  $m$  and radius  $R$ , initially resting on a horizontal surface. The system is submitted to an external horizontal force, provided by a driving mechanism, through a thin rod attached to a fixed point ( $P$ ) on the disk, around which the whole body can rotate freely. The driving apparatus takes the disk from rest and makes the point  $P$  follow a uniform circular trajectory of radius  $d$  around a fixed origin ( $O$ ) with angular frequency  $\omega$  [see Fig. 2(a)]. For definiteness we assume the rotation to be counterclockwise and, without loss of generality, we use a coordinate system for which the point  $P$  lies on the positive  $x$  axis at  $t = 0$ .

For later times we denote the position vector of  $P$  by  $\mathbf{d}$  and the vector locating the c.m. by  $\mathbf{r}$ . Since the disk is assumed to be perfectly rigid,  $P$  is always a distance  $l$  away from the c.m. The relative position of these two points is given by the vector

\*pablo@df.ufpe.br

†parisio@df.ufpe.br

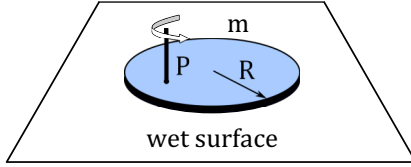


FIG. 1. (Color online) Pictorial representation of the proposed model system.

$\mathbf{l}$ , as shown in Fig. 2(a). Finally, the angle between the  $x$  axis and the line connecting the c.m. and  $P$  is denoted by  $\phi$ . The variables  $\mathbf{r}$  and  $\phi$  completely specify the position of the disk, while  $\omega$  reflects the strength of driving.

In a previous work the scenario of negligible friction was assumed [4]. Here we remove this restriction by considering that a thin layer of fluid exists between the disk and the horizontal surface, giving rise to wet friction. This amounts to viscous forces and torques that are proportional to the local relative velocity between the surfaces.

### A. Viscous friction

The overall viscous force acting on the disk is given by the surface integral

$$\mathbf{F} = -\frac{b}{\pi R^2} \int_{\text{disk}} \dot{\mathbf{s}} \rho d\alpha d\rho, \quad (1)$$

where  $b$  is the drag constant and  $\mathbf{s}$  is the vector that locates the element of area  $\rho d\alpha d\rho$  [see Fig. 2(b)]. Taking into account the constraints  $\mathbf{r} + \mathbf{l} = \mathbf{d}$  and  $\mathbf{r} + \boldsymbol{\rho} = \mathbf{s}$ , the result reduces to that of a rectilinear, irrotational, motion of the disk:  $\mathbf{F} = -b\dot{\mathbf{r}}$ . In addition, the forces on each element of area give rise to a torque:

$$\mathbf{T} = -\frac{b}{\pi R^2} \int_{\text{disk}} \mathbf{s} \times \dot{\mathbf{s}} \rho d\alpha d\rho = -b\mathbf{r} \times \dot{\mathbf{r}} - \frac{bR^2}{2} \dot{\phi} \hat{z}, \quad (2)$$

where  $\phi$  is the angle between the vector  $\mathbf{l}$  and the  $x$  axis, and  $\hat{z}$  is the unit vector perpendicular to the plane of motion. Plugging these expressions into Newton's second law and eliminating the c.m. degrees of freedom we get

$$I_P \ddot{\phi} + b \left( l^2 + \frac{R^2}{2} \right) \dot{\phi} - mdl\omega^2 \sin(\phi - \omega t) - bdl\omega \cos(\phi - \omega t) = 0, \quad (3)$$

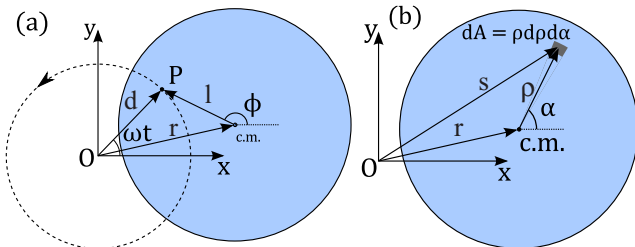


FIG. 2. (Color online) Schematic upper view of the system where the relevant geometric quantities are depicted (a), and integration variables for the calculation of the viscous force and torque (b).

where  $I_P$  is the moment of inertia relative to the pivot point  $P$ . By writing

$$\theta = \phi - \omega t + \arctan\left(\frac{b}{m\omega}\right) + \pi, \quad (4)$$

the equation of motion considerably simplifies to

$$\mathcal{S} \frac{\ddot{\theta}}{\omega^2} + \frac{\dot{\theta}}{\omega} + \frac{\sqrt{\mathcal{S}^2 + 1}}{H} \sin \theta + 1 = 0, \quad (5)$$

where the parameter

$$H = \frac{L^2 + 1/2}{DL}, \quad (6)$$

with  $D = d/R \in [0, \infty)$  and  $L = l/R \in [0, 1]$ , contains all the relevant information on the scale-free geometry of the system, and  $\mathcal{S} = m\omega/b$  gives the relative strength of the inertial and driving versus viscous forces on the disk. Although in our calculations we will use Eq. (5), it is possible to obtain a formally simpler equation by using the dimensionless time  $\tau = (\mathcal{S}A/\omega)t$ , with  $A = H^{1/2}(\mathcal{S}\sqrt{\mathcal{S}^2 + 1})^{-1/2}$ . The resulting two-parameter differential equation reads

$$\frac{d^2\theta}{d\tau^2} + \mathcal{A} \frac{d\theta}{d\tau} + \sin \theta + \mathcal{S}A^2 = 0. \quad (7)$$

The cost is that  $\mathcal{A}$  is an involved mixture of geometry, inertia, driving, and viscosity. From Eq. (7) we see that our problem can be mapped into the dynamics of a pendulum immersed in a fluid and subjected to a constant torque [15]. It is interesting to note that a number of quite distinct physical systems are, in some regimes, described by the very equation (7). Examples are the dynamics of the phase difference between the collective wave functions through a Josephson junction [16,17], the excitable behavior of microparticles under the action of an optical torque wrench [18], and alternating currents in electrical devices [19,20]. It is, however, important to note two points. First, the physical quantity we are interested in, which defines reverse or normal rotations, is  $\phi$  and not  $\theta$ . Second, to completely characterize the problem, we must provide physically valid initial conditions. In the present case it is natural to assume that, at first, the disk is resting on the horizontal surface, and at a certain instant, say  $t = 0$ , the driving apparatus is turned on. If the driving mechanism is robust enough, we can assume that this initial dynamics is impulsive, that is, the pivot point is taken from rest to the final constant angular velocity in a time interval much shorter than any other time scale in the problem. Under these conditions it has been shown in Ref. [4] that, given the initial angle of the static disk, the angular velocity it acquires immediately after the driving apparatus is switched on is

$$\dot{\phi}_0 = \frac{\omega}{H} \cos \phi_0. \quad (8)$$

Replacing this relation in the equation of motion we also find that  $\ddot{\phi}_0 = (\omega^2/H) \sin \phi_0$ . In the original derivation the friction was not taken into account. This, however, does not affect the above result due to the hypothesis of impulsivity.

To illustrate the restrictions imposed by the previous relation we remark that the system studied in Ref. [15] presents the interesting behavior of excitability, namely, the existence of a dynamical regime with sharp spikes in  $\theta(t)$ .

The authors observe this phenomenon for a condition that, in our notation, reads  $\omega > (b/m)\sqrt{H^2 - 1}$  with initial condition  $\dot{\theta}_0 = 0$ , and arbitrary  $\theta_0$ . Replacing this condition in Eq. (8) we get  $H = \cos \phi_0$ , which implies  $H \leq 1$ , leading to a negative argument in the square root. Therefore, our system, does not present the excitability observed in Ref. [15] due to the initial conditions we are concerned with.

### B. Limiting cases

We start this section with a summary of the main conclusions obtained in the frictionless ( $b = 0$ ) case [4]. It was found that a regime of perennial reverse rotations is possible for an interval of initial angles  $\{\pi - \phi_B, \pi + \phi_B\}$  centered at  $\pi$  (the subscript  $B$  stands for “boundary”), provided that the geometrical constraint

$$H < 0.793 \quad (9)$$

is satisfied. In fact, it can be derived from Eqs. (5) and (11) of [4] that, with a fixed angle  $\phi_B$ , the critical value of  $H$  below which reverse rotations occur can be determined by the solution of the transcendental equation

$$K\left(\frac{2\sqrt{H}}{\sqrt{H^2 + 2H + \cos^2 \phi_B}}\right) = \frac{\pi}{2H}\sqrt{H^2 + 2H + \cos^2 \phi_B}, \quad (10)$$

where  $K$  denotes the complete elliptic function of the first kind. For  $\phi_B = 0$ , the only angle leading to reverse dynamics is  $\phi_0 = \pi$ . In this case the above equation reduces to  $K[2\sqrt{H}/(H+1)] = \pi(H+1)/2H$ , whose nontrivial solution is  $H_c = 0.793$ . For all other situations, where  $\phi_B \neq 0$ ,  $H_c$  assumes smaller values. For  $H > 0.793$  no initial condition may develop a reverse rotation. Note that this necessary and sufficient condition does not depend on the driving frequency  $\omega$ , on the mass  $m$ , or on the absolute values of the lengths  $d$ ,  $l$ , and  $R$ . Initial conditions that do not satisfy the previous requirements lead either to a permanent regime of normal rotations or, in the boundary between the two regimes, to an oscillatory motion with a vanishing average of  $\phi$  as time goes by (see Fig. 3 of Ref. [4]).

In the opposite limit  $b \rightarrow \infty$ , Eq. (5) becomes

$$\dot{\theta} + \frac{\omega}{H} \sin \theta + \omega = 0, \quad (11)$$

whose fixed points are given by  $\sin \theta^* = -H$  and  $\cos \theta^* = \pm\sqrt{1 - H^2}$ . Let us summarize the three qualitatively distinct solutions of this equation [17]. (i) If  $H < 1$  we have two fixed points in the interval  $[0, 2\pi)$ , the stable one having  $\cos \theta^* > 0$ , and no oscillation. (ii) For  $H = 1$  we have a saddle-node bifurcation with no oscillation for any finite time. (iii) If  $H > 1$  there are no fixed points and the system oscillates with a period given by

$$T = \frac{2\pi}{\omega\sqrt{1 - H^{-2}}} \geq \frac{2\pi}{\omega}. \quad (12)$$

The important point is that, by inspecting Eq. (4), we note that, in any case,  $\phi(t)$  is an increasing function of time, on average, thus, presenting normal rotations only.

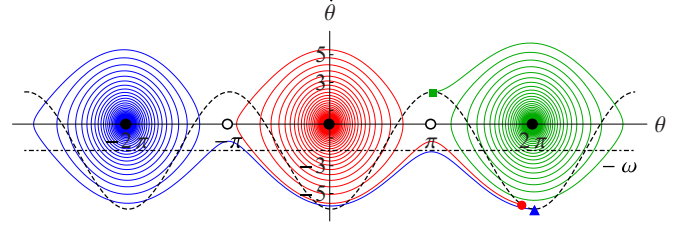


FIG. 3. (Color online) Phase-space trajectories for three different initial conditions. More details are given in the text.

Therefore, we conclude that while in the frictionless case reverse rotations may occur, they are forbidden in the high-viscosity limit. The question arises what happens in between?

### III. ARBITRARY VISCOSITY

Although a closed analytical solution for our problem with arbitrary viscosity is not available, we can establish the stationary points and their stability properties before going into numerical solutions. By setting  $\dot{\theta} = 0$  and  $\theta = 0$  in Eq. (5) we obtain stable fixed points satisfying

$$\theta^* = -\arcsin\left(\frac{H}{\sqrt{S+1}}\right) \pm 2n\pi, \quad (13)$$

with  $n = 0, 1, 2, \dots$ . The unstable stationary points are given by  $\pi - \theta^*$ . Our numerical investigation for intermediate values of the parameter  $b/m$  begins with some typical trajectories in the plane  $\theta$ - $\dot{\theta}$ . We employed the auxiliary variables directly because only in terms of them does the equation of motion not contain time explicitly. In Fig. 3 we show a phase-space diagram for three initial conditions  $\theta_0 \approx 2\pi$  ( $\phi_0 = \pi$ ) for the triangle,  $\theta_0 \approx \pi$  ( $\phi_0 = 0$ ) for the square, and  $\theta_0 = 2\pi - \pi/8$  ( $\phi_0 = \pi - \pi/8$ ) for the circle, with the corresponding initial velocities given by relation (8), represented by the dashed line in the diagram. The other parameters are as follows:  $b/m = 0.09$ ,  $\omega = 1.9$ , and  $H = 0.45$ . This leads to  $\sin \theta^* = -0.021$  and  $\theta^* \approx -1^\circ, 2^\circ$ . The horizontal dash-dotted line represents the negative of the driving angular frequency  $\omega$ . Recall that, to have a reverse rotation [ $\dot{\phi}(t) < 0$  over a time scale of  $2\pi/\omega$ ], we must get  $\langle \dot{\theta}(t) \rangle < -\omega$  over a time scale of  $2\pi/\omega$ . We note that the first initial condition immediately leads to normal rotation, for the second condition a reverse behavior develops during a single cycle, while the third initial condition presents two cycles of reverse rotation before spiraling to the leftmost stable fixed point.

Going to the physical variable  $\phi$ , the first important thing to note is as follows. For every initial condition that started to develop a reverse rotation, after some time, the spin invariably flips to a regime of prograde rotation for any  $b \neq 0$ . This can be understood by noting that the oscillations in  $\phi(t)$  eventually fade out, with  $\dot{\phi} \rightarrow 0$  for sufficiently long times, an effect observed in all investigated configurations. When this regime is reached the equation of motion becomes identical to Eq. (11), for which reverse rotations have been shown to be absent. Therefore, at some moment, reverse dynamics is replaced by normal rotation, and the smaller the drag the longer the flip time  $t_f$ , which is determined by the global minimum of  $\phi(t)$ . In Fig. 4 we show  $\phi$  as a function of  $t$  for  $\omega = 0.2 \text{ rad s}^{-1}$ ,

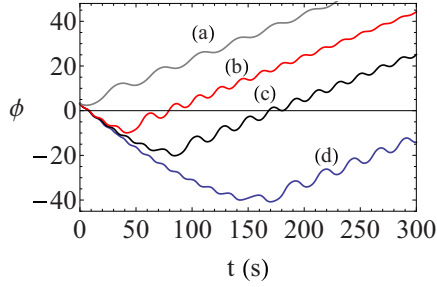


FIG. 4. (Color online) The angle  $\phi$  as a function of  $t$  for  $\omega = 0.2 \text{ rad s}^{-1}$  and  $\phi_0 = \pi$ . Curve (a) presents a prograde dynamics, as expected, since  $H = 1.0 > H_c$ . For  $H = 0.3$  and  $b/m = 0.014 \text{ s}^{-1}$  (b),  $b/m = 0.008 \text{ s}^{-1}$  (c), and  $b/m = 0.004 \text{ s}^{-1}$  (d), reverse rotations are observed.

and initial condition  $\phi_0 = \pi$  (the most favorable to reverse rotations). The first curve (a) occurs for  $H = 1.0$  (no reverse motion) and  $b/m = 0.008 \text{ s}^{-1}$ . The three other curves refer to  $H = 0.3$  with distinct values of the drag parameter:  $b/m = 0.014 \text{ s}^{-1}$  (b),  $b/m = 0.008 \text{ s}^{-1}$  (c), and  $b/m = 0.004 \text{ s}^{-1}$  (d). We therefore conclude that no steady reverse rotation is allowed for any finite value of  $b/m$ . This regime, however, can exist as a transient that lasts longer for smaller values of viscosity.

The lifetime of reverse rotations must be null in the limit of high viscosity and has to diverge in the frictionless regime. Dimensional analysis leads us to infer that, if this divergence is described by a power law, then we should have  $t_f \sim \omega^{\gamma-1} (b/m)^{-\gamma}$ . In Fig. 5 we record  $t_f$  as a function of  $b/m$  in a log-log plot. The discontinuities happen when the global minimum jumps between neighboring local minima. Despite these jumps, a linear backbone is noticeable in a broad range of viscosity values, and a power-law divergence in the low-viscosity limit is clear. The obtained relation is

$$t_f \sim \left(\frac{b}{m}\right)^{-1} \quad (14)$$

which we found to be asymptotically independent of  $\omega$  [21]. The variation of the drag parameter has a much less dramatic

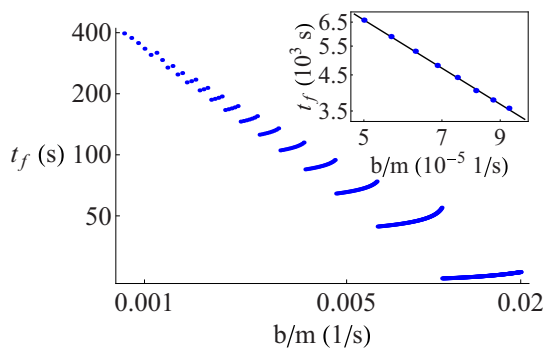


FIG. 5. (Color online) Log-log plot of the flip time  $t_f$ , as a function  $b/m$ , showing a power-law behavior in the regime of low viscosity. The discontinuities are due to the passage of the global minimum through consecutive local minima. The inset depicts a region of much weaker viscosity.

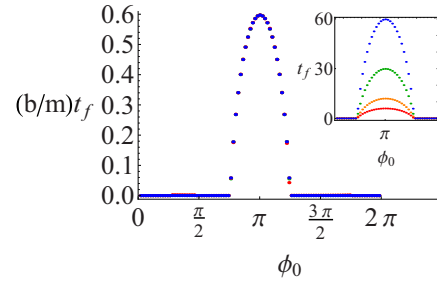


FIG. 6. (Color online) Dimensionless flip time  $(b/m)t_f$  as a function of the initial condition  $\phi_0$  for four different values of  $b/m$ . The plots completely overlap. The inset shows the uncollapsed curves of  $t_f$  against  $\phi_0$ . Further details are given in the text.

effect on the regime of normal rotations, the only difference being the rate at which the amplitude of the oscillations in  $\phi(t)$  goes to zero.

In spite of this, we verified that the initial conditions that lead to reverse rotations in the case of vanishing viscosity are the same that give rise to the reverse transient, the interval  $\{\pi - \phi_B, \pi + \phi_B\}$  being insensitive to the value of  $b$ . This is expected due to the impulsive nature of the initial energy input. In addition, due to relation (14) we suspected that the dependence of  $t_f$  with  $\phi_0$  might be universal with respect to the dimensionless time  $(b/m)t_f$ . This is indeed the case, as Fig. 6 shows for different values of  $b/m$ . In the inset we plot the uncollapsed curves of  $t_f$  alone against  $\phi_0$ . We used a high angular velocity  $\omega = 200 \text{ rad s}^{-1}$ , in order to suppress oscillations and make the plot clearer. For lower values of  $\omega$  the results are qualitatively the same and Fig. 6 would represent the envelope of the actual plots. The other parameters employed are  $H = 0.3$ , and  $b/m = 0.1 \text{ s}^{-1}$  (a),  $b/m = 0.2 \text{ s}^{-1}$  (b),  $b/m = 0.5 \text{ s}^{-1}$  (c), and  $b/m = 1.0 \text{ s}^{-1}$  (d). The invariant value of  $\phi_B$  is approximately  $3\pi/5$ .

We now turn our attention to the geometric parameter defined in Eq. (6). In the absence of friction, we found that reverse rotations are possible only if  $H < 0.793 = H_c(0)$ , according to (9). Although perennial reverse rotations are not present for  $b \neq 0$ , one may ask which values of  $H$  allow for transient reverse behavior. In Fig. 7 we display the maximum value of  $H$  below which reverse dynamics can occur as a function of  $b/m\omega$ , with  $\phi_0 = \pi$ . Interestingly enough, the

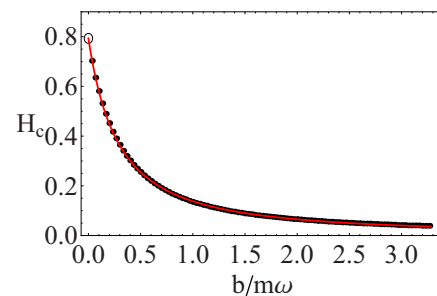


FIG. 7. (Color online) Critical geometric parameter  $H_c$  versus the dimensionless variable  $\mathcal{S}^{-1} = b/m\omega$ .  $H_c$  falls off following a  $q$ -exponential function with  $q = 1.7$  for  $\phi_0 = \pi$ . The open circle represents  $H_c = 0.793$ .

numerical data are very well described by a  $q$ -exponential function:

$$H_c(b/m\omega) = H_c(0) \left[ 1 - \lambda(1 - q) \left( \frac{b}{m\omega} \right) \right]^{1/(1-q)}, \quad (15)$$

with  $q = 1.7$  and  $\lambda = 3.47$ . When  $\phi_0$  departs from  $\pi$ , both the values of  $q$  and  $H_c(0)$  tend to decrease. For  $\phi_0 = 2.5$ , e.g., we get  $q \approx 1.5$  and  $\lambda \approx 2.23$ , while  $H_c(0)$  drops considerably to 0.40. The values of  $H_c(0)$  quickly become very restrictive to reverse motion as, for example,  $\phi_0 = 2.0$ , leading to  $H_c(0) \approx 0.09$ . For  $L = 0.5$ , such a condition on  $H$  would be satisfied only for  $D \geq 17$ , hindering in practice the occurrence of reverse rotations. We thus see that increasing wet friction not only decreases the lifetime of reverse rotations, but also reduces the region in the space of parameters  $L$  and  $D$  for which they are possible.

#### IV. CONCLUSIONS

In this work we studied the influence of wet friction in the circularly driven motion of a disk. We found that the spinning dynamics of the disk is given by a combination (competition) between a uniform motion and a pendular motion (associated with a pendulum immersed in a viscous fluid and acted upon by a constant torque); see Eq. (7). While in the frictionless case reverse rotations may exist in steady regimes, for any finite value of viscous damping, this behavior becomes a transient, thus having a finite lifetime. This transient have been completely characterized: (i) Its lifetime follows a power law with  $t_f \sim m/b$ ; (ii) the presence of viscosity reduces the possible geometric configurations that lead to rotations that are initially reverse due to the fall of  $H_c$ , according to a  $q$ -exponential; (iii) however, the interval of initial conditions  $\phi_0$  that leads to retrograde behavior is

insensitive to the value of  $b$ . In fact the whole shape of the function  $(b/m)t_f(\phi_0)$  is independent of the dragging. A natural extension of the present work is to consider the analogous situation with Coulombian (dry) friction. This leads to a more complex equation of motion involving elliptic functions of intricate arguments and requires a full numerical treatment.

Regarding the appearance of a  $q$ -exponential (introduced in the context of statistical physics by Tsallis [22]) describing the behavior of a critical parameter in a situation that does not explicitly involve statistics, it might look unexpected. Although the classical foundations of nonextensive statistical mechanics may be formally understood via generalizations of the Langevin equation [23], where viscous friction plays an essential role, one cannot easily relate our result to this kind of microscopic description. A more plausible possibility is simply attributed to the ability of  $q$ -exponentials to fit a broad class of decreasing functions. Whether Eq. (15) is a pure mathematical fact, as we strongly believe, or has a deeper statistical explanation, is a matter to be investigated. The same observation is valid for the range of values we obtained for  $q$ , which also appears in the statistical studies of complex systems, e.g., in the distribution of urban agglomerates in Brazil and the USA [24].

#### ACKNOWLEDGMENTS

The authors thank Tiago Araújo and Victor Pedrosa for many stimulating discussions on this work. Financial support from Conselho Nacional de Desenvolvimento Científico e Tecnológico (CNPq), Coordenação de Aperfeiçoamento de Pessoal de Nível Superior (CAPES), and Fundação de Amparo à Ciência e Tecnologia do Estado de Pernambuco (FACEPE) (Grant No. APQ-1415-1.05/10) is acknowledged.

- 
- [1] Z. Farkas, G. Bartels, T. Unger, and D. E. Wolf, *Phys. Rev. Lett.* **90**, 248302 (2003).
  - [2] P. D. Weidman and C. P. Malhotra, *Phys. Rev. Lett.* **95**, 264303 (2005).
  - [3] P. D. Weidman and C. P. Malhotra, *Physica D* **233**, 1 (2007).
  - [4] F. Parisio, *Phys. Rev. E* **78**, 055601(R) (2008).
  - [5] See, for example, <http://solarsystem.nasa.gov/planets>.
  - [6] A. C. M. Correia and J. Laskar, *Nature (London)* **411**, 767 (2001).
  - [7] A. C. M. Correia, J. Laskar, and O. N. de Surgy, *Icarus* **163**, 1 (2003).
  - [8] J. R. T. Seddon and T. Mullin, *Phys. Fluids* **18**, 041703 (2006).
  - [9] C. Sun *et al.*, *J. Fluid Mech.* **664**, 150 (2010).
  - [10] A. Merlen and C. Frankiewicz, *J. Fluid Mech.* **685**, 461 (2011).
  - [11] K. Yoshida and K. Sato, *Int. J. Non-Linear Mech.* **33**, 819 (1998).
  - [12] S. DeCamilo, K. Brockwell, and W. Dmochowsky, *Tribol. Trans.* **49**, 305 (2006).
  - [13] S. L. Waters *et al.*, *IMA J. Math. Med. Biol.* **23**, 311 (2006); L. J. Cummings and S. L. Waters, *ibid.* **24**, 169 (2007).
  - [14] L. J. Cummings *et al.*, *Biotechnol. Bioeng.* **104**, 1224 (2009).
  - [15] P. Couillet *et al.*, *Am. J. Phys.* **73**, 1122 (2005).
  - [16] G. L. Baker, *The Pendulum: A Case Study in Physics* (Oxford University Press, Oxford, 2005).
  - [17] S. H. Strogatz, *Nonlinear Dynamics and Chaos* (Westview, Cambridge, MA, 2000).
  - [18] F. Pedaci *et al.*, *Nat. Phys.* **7**, 259 (2011).
  - [19] F. Tricomi, *Ann. Sc. Norm. Super. Pisa, Class. Sci.* **2**, 1 (1933).
  - [20] G. A. Leonov, *Mathematical Problems of Control Theory* (World Scientific, Singapore, 2001).
  - [21] We found a weak oscillatory dependence of  $t_f$  on angular velocity for small values of  $\omega$ . However, also in this situation we obtain  $\gamma = 1$ .
  - [22] C. Tsallis, *J. Stat. Phys.* **52**, 479 (1988).
  - [23] C. Beck, *Phys. Rev. Lett.* **87**, 180601 (2001).
  - [24] L. C. Malacarne, R. S. Mendes, and E. K. Lenzi, *Phys. Rev. E* **65**, 017106 (2001).